Original citation:
Lu, Yi, Wang, Xiayang, Higgins, Matthew D., Noel, Adam, Neophytou, Neophytos and Leeson, Mark S.. (2016) Energy requirements of error correction codes in diffusion-based molecular communication systems. Nano Communication Networks.

Permanent WRAP URL:
http://wrap.warwick.ac.uk/81742

Copyright and reuse:
The Warwick Research Archive Portal (WRAP) makes this work by researchers of the University of Warwick available open access under the following conditions. Copyright © and all moral rights to the version of the paper presented here belong to the individual author(s) and/or other copyright owners. To the extent reasonable and practicable the material made available in WRAP has been checked for eligibility before being made available.

Copies of full items can be used for personal research or study, educational, or not-for-profit purposes without prior permission or charge. Provided that the authors, title and full bibliographic details are credited, a hyperlink and/or URL is given for the original metadata page and the content is not changed in any way.

Publisher's statement:
© 2016, Elsevier. Licensed under the Creative Commons Attribution-NonCommercial-NoDerivatives 4.0 International http://creativecommons.org/licenses/by-nc-nd/4.0/

A note on versions:
The version presented here may differ from the published version or, version of record, if you wish to cite this item you are advised to consult the publisher's version. Please see the 'permanent WRAP URL' above for details on accessing the published version and note that access may require a subscription.

For more information, please contact the WRAP Team at: wrap@warwick.ac.uk

warwick.ac.uk/lib-publications

Energy Requirements of Error Correction Codes in Diffusion-Based Molecular Communication Systems

Yi Lu[a], Xiayang Wang[a], Matthew D. Higgins [b,*], Adam Noel[c], Neophytos Neophytou[a], Mark. S. Leeson[a]

[a]*School of Engineering, University of Warwick, Coventry, CV4 7AL, UK*
[b]*WMG, University of Warwick, Coventry, CV4 7AL, UK*
[c]*School of Electrical Engineering and Computer Science, University of Ottawa, Ottawa, ON K1N 6N5, Canada*

Abstract

Molecular Communications is a promising area with significant potential applications. To enhance the reliability of the transmission process, self-orthogonal convolutional codes (SOCCs) are proposed and investigated with respect to both bit error rate (BER) and energy efficiency. The codes are compared to both an un-coded system and one that employs Hamming codes to show that they can provide a benefit for molecular communication systems. The influence of the channel memory is also analysed in this paper. In addition, taking into account the extra energy required to implement the coding, the critical distance is investigated as another performance metric for nano-to-nano device communication, nano-to-macro device communication and macro-to-nano device communication. Considering the transmission distance and the operating BER of the designed system, the designer can determine whether the use of coding is beneficial or which code better suits the system.

Keywords: Diffusion Channel, Energy Requirements, Hamming Codes, Molecular Communications, SOCCs

1. Introduction

With the ever increasing developments in nanotechnology, the number of potential applications requiring connectivity between each of the nano-devices has risen accordingly. Furthermore, in order to establish, or improve these nano-communication systems and associated applications, knowledge about the interaction of the nano-devices with the classical network is becoming more commonly considered within the Internet of Nano Things (IoNT) [1] paradigm. One of the key applications proposed as part of this IoNT is that of intra-body health monitoring where the channel is based upon the diffusion of molecules.

An example is shown in Figure 1 which illustrates the simplified structure of a health monitoring system that may comprise two sizes of device. A nano-sensor or nano-robot may be present, which is essentially a device whose components are all at the scale of a nanometre. For example, drug delivery mechanisms [2], or targeted surgery sensors [3]. Also present may be macro-devices which are manufactured using traditional micro-scale components, such as those found in micro-electro-mechanical systems (MEMS) [4]. These macro devices are not designed to be
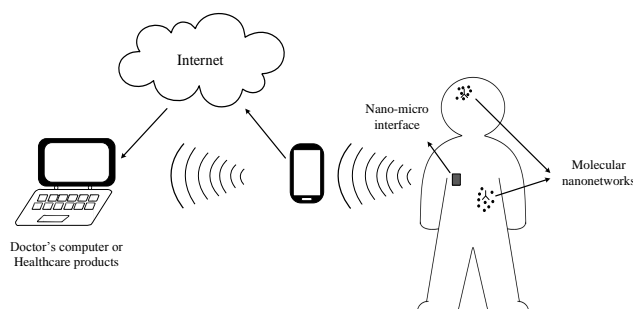

Figure 1: A simplified health-care monitoring system design.

mobile and are most likely found on (or just under) the skin. In essence, the macro-device acts as the gateway between the nano-device and the wider network or Internet.

Already, with this simple scenario, a range of issues can be identified between the patients' nano-sensor/device and the doctor. Not only are there numerous physical layers to accommodate, but there are likely to be different requirements in the data and control aspects at each stage, some of which will be well-defined, but others will not. For example, the TCP/IP of the internet, or one of the numerous IEEE802.x Wi-Fi standards, are not up for negotiation, whilst the protocols required for the links between nano- and macro- devices, are still at the debate stage within the literature [5] [6], [7], [8], [9].

There will also be issues regarding the power availability. It has been claimed that the nano-devices will most likely

---

*Corresponding author

Email addresses: `Yi.Lu@warwick.ac.uk` (Yi Lu), `xiayang.wang@warwick.ac.uk` (Xiayang Wang), `m.higgins@warwick.ac.uk` (Matthew D. Higgins), `anoel2@uottawa.ca` (Adam Noel), `n.neophytou@warwick.ac.uk` (Neophytos Neophytou), `mark.leeson@warwick.ac.uk` (Mark. S. Leeson)

have to work in the nW, if not pW region [10], whilst the macro-devices are essentially unconstrained in comparison. Overarching all of this are issues regarding data integrity and security which for medical applications are likely to define the level of social acceptance [11].

This paper focuses on the link between the nano-device and the nano-macro interface, where specifically, it is assumed that the link be based upon a molecular diffusion [4] process. As is true for most, if not all, communications systems, it is vital that the data transmission is both efficient and reliable. Thus, the use of Error Correction Codes (ECCs) has become an essential part in the communication system design.

The first attempt in analysing the benefits of coding techniques in a molecular communication system was presented by Leeson and Higgins in [12] and [13], where the Hamming codes were implemented. Crucially, the results took account of the overall complexity of the encoding and decoding process such that the amount of energy that would be required was also considered, which then allowed the determination of the critical distance [14]. Further work followed in [15] focusing on the need to introduce simple codes due to this issue of energy use. Additional codes, including High-order Hamming Codes [16], Minimum Energy Codes [17], Low Density Parity Check Codes and Reed-Muller Codes [18] have also been investigated. In each of the aforementioned investigations, code simplicity, system performance and energy requirements became the critical areas when considering the choice of coding techniques within molecular communication systems. It can also be seen that all codes were block codes.

There is another class of ECC besides block codes, known as convolutional codes. One such code is the self-orthogonal convolutional code (SOCC). A SOCC is a kind of convolutional code that has a property of being easy to implement thus satisfying one of the key design requirements of code simplicity [19], [20]. Further motivation of this study is that this kind of convolutional code has been shown to have an equal, or superior performance to block codes in low cost and low complexity applications. Numerous examples can be found detailing their competitiveness in practical applications [21], [22], [23], [24].

The proposal to introduce the use of SOCCs in molecular communication systems was first introduced by Lu *et al.* [25]. However, two key observations could be made about the work. Firstly, the channel model implemented could only account for ISI under the assumption that molecules were not removed from the channel after their reception, i.e. the use of a non-absorbing receiver. Secondly, the results were then limited to cover only the effects of ISI from one previous symbol. Thirdly, the work only considered nano-to-nano links which as noted above limited the overall impact of the work.

Since the original publication of [25], the community has more commonly moved to adopt a model that assumes absorbing receivers and as such, the channel model of [26] will be used herein. The use of this model is an advance to
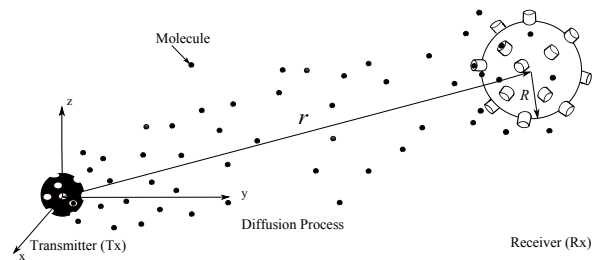

Figure 2: The diffusion-based system considered in this work.

the field as no other paper on the topic of error correction codes within molecular communications currently assumes an absorbing receiver. Through using this model, this paper aims to provide a derivation of the BER for both coded and uncoded systems. This allows for this work to also be used as a guide to how the results are formed and should therefore act as a tutorial to assist the reader in applying new codes to their own specific future systems.

Next, the use of SOCCs is investigated as an candidate code, and their performance, in terms of coding gain and critical distance is evaluated against a system that is uncoded or uses Hamming codes. Finally, to enhance the impact of this investigation, making it applicable to as many elements of a system, such as the one in Figure 1, the results are the expanded to include communications links between nano-devices and macro-devices by incorporating assumptions of their respective power budgets.

The remainder of the paper is organised as follows. Section 2 describes the communications channel model. In Section 3, the energy model of molecular communications is discussed. The theoretical and implementation aspects of Hamming codes and SOCCs are then shown in Section 4 which also provides the reader with a definitive set of equations needed to calculate the energy requirements. Section 5 then provides the numerical results, followed by the conclusions in Section 6.

2. The Communications Channel Model

In this work, the information is transmitted from the transmitter (T_X) to the receiver (R_X) by a certain number of diffused molecules. A three dimensional diffusion-based communications system is depicted in Figure 2, where the propagation of molecules from the T_X to the R_X is modelled by Brownian motion. In this model, the R_X has a molecule capture probability $P(r,t)$ given by [27, Equation 2]:

$$P(r,t) = \frac{R}{r}\text{erfc}\left(\frac{r-R}{2\sqrt{Dt}}\right),\tag{1}$$

where r is the distance between the initial position (the centre of the T_X) of the molecule and the centre of the R_X, in μm, t is time in s. R is the radius of the R_X, in μm, and D is the diffusion coefficient, in μm^{2}s^{-1}.

2

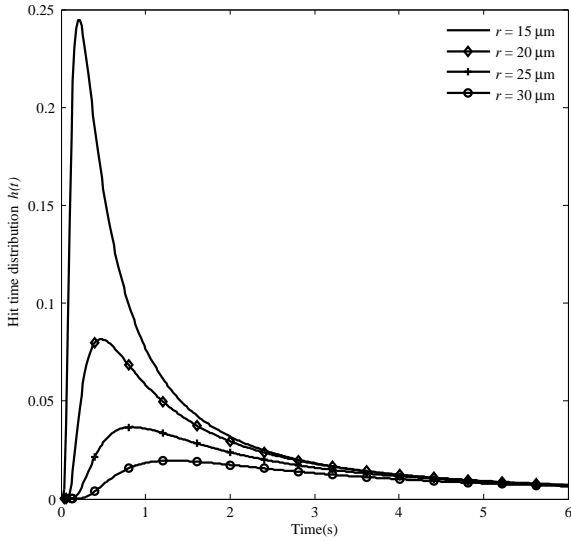Figure 3: Hit time distribution for different distance $r = 15$ μm, 20 μm, 25 μm, 30 μm.

The molecules released from the T_X cannot be guaranteed to reach the R_X within one time slot, so the probability that an information molecule arrives at the R_X at a certain time t is introduced, which can be denoted as the hit time distribution $h(t)$ that can be obtained by differentiating the capture probability, $P(r, t)$ in (1), with respect to time as:

$$h\left(t\right) = \frac{Rd}{2r\sqrt{\pi D}t^{3/2}}e^{\left(-\frac{d^2}{4Dt}\right)}, \qquad (2)$$

where $d = r - R$. In this paper, $R = 5$ μm and $D = 79.4$ μm^{2}s^{-1} are assumed for ease of comparison with the work in [12] and [13]. Figure 3 shows examples of the hit time distribution.

The communication channel used here is assumed to be a binary channel. The transmitted information is represented in binary form, where this binary value represents a concentration of molecules transmitted between these nano-devices with one symbol in each time slot t_s. For example, '1' represents a specific number of molecules released from the T_X, and '0' represents no molecules released. At the R_X, if the number of information molecules arriving at the R_X exceeds a threshold τ, the symbol is denoted as '1'; otherwise, it is denoted as '0' [28]. For different numbers of molecules per bit, the τ is different and can be obtained by minimizing the BER. However, errors may be introduced due to the effects of ISI which are caused by the remaining molecules from the previous symbols. In this paper, the current symbol can be treated as being affected by I previous symbols, where I is denoted as ISI length.

At the T_X, N information molecules are released as an impulse at the start of the symbol duration time, and among these N molecules that are sent in the current time slot, the number of molecules received by the R_X, N_0, follow a binomial distribution [29, Equation 7]:

$$N_0 \sim B\left(N, P\left(r, t_s\right)\right). \qquad (3)$$

When N is large enough, a binomial distribution $B(N, P)$ can be approximated by a normal distribution $\mathcal{N}(NP, NP(1 - P))$, thus:

$$N_0 \sim \mathcal{N}\left(NP\left(r, t_s\right), NP\left(r, t_s\right)\left(1 - P\left(r, t_s\right)\right)\right). \qquad (4)$$

The values of t_s, for different distances r, are selected by the time at which 60% molecules arrive at the R_X [29].

The molecules coming from the previous time slots may arrive during the current time slot. Considering the molecules emitted at the start of the ith time slot before the current one, the number of molecules received in the current time slot among these remaining molecules is given by [26, Equation 3]:

$$N_i \sim \mathcal{B}\left(N, P_{i+1} - P_i\right)$$
$$\sim \mathcal{N}\left(N\left(P_{i+1} - P_i\right), N\left(P_{i+1} - P_i\right)\left(1 - P_{i+1} + P_i\right)\right), \qquad (5)$$

where $P_i = P(r, i \cdot t_s)$ and $i = 0, 1, 2, ..., I$. When $i = 0$, $N_i = N_0$.

Thus, the total number of molecules received in the current time slot, N_c, comprises the number of received molecules for the current symbol and all I previous symbols:

$$N_c = \sum_{i=0}^{I} a_{c-i} N_i$$
$$\sim \sum_{i=0}^{I} a_{c-i} \mathcal{N}\left(N\left(P_{i+1} - P_i\right), N\left(P_{i+1} - P_i\right)\left(1 - P_{i+1} + P_i\right)\right), \qquad (6)$$

where $\{a_{c-i}, i = 0, 1, 2, ..., I\}$ represents the transmitted information symbols which includes current and all previous I symbols.

Considering the ISI, the error patterns can be obtained by the different permutations of the previous information symbols, so the number of error patterns is 2^I and for each of these, $j = \{1, 2, ..., 2^I\}$ is the error pattern index. Thus, N_c can be rewritten as $N_{c,j}$:

$$N_{c,j} = \sum_{i=0}^{I} a_{c-i,j} N_i$$
$$\sim \sum_{i=0}^{I} a_{c-i,j} \mathcal{N}\left(N\left(P_{i+1} - P_i\right), N\left(P_{i+1} - P_i\right)\left(1 - P_{i+1} + P_i\right)\right), \qquad (7)$$

An error occurs when there is a difference between the symbol that was sent and that received in the current time slot. The error can be represented in two cases. Firstly, when a '0' is transmitted, but '1' is received, and secondly, when a '1' is transmitted, but '0' is received.

The error probability for the first case shows that the received molecules exceed τ, which is:

$$P_{01,j} = \frac{1}{2^I}\mathrm{P}\left(N_{c,j} > \tau\right)$$
$$= \frac{1}{2^I}\mathrm{P}\left(\sum_{i=0}^{I} a_{c-i,j} N_i > \tau\right), \qquad (8)$$

3

Table 1: Error probabilities for different error patterns for $I = 2$.

The previous symbols		Error probabilities: transmit '0', receive '1'	Error probabilities: transmit '1', receive '0'
a_{c-2}	a_{c-1}	$P_{01,j}$	$P_{10,j}$
0	0		$Q\left(\frac{NP_1-\tau}{\sqrt{NP_1(1-P_1)}}\right)$
0	1	$Q\left(\frac{\tau-N(P_2-P_1)}{\sqrt{N(P_2-P_1)(1-P_2+P_1)}}\right)$	$Q\left(\frac{NP_2-\tau}{\sqrt{N((P_2-P_1)(1-P_2+P_1)+P_1(1-P_1))}}\right)$
1	0	$Q\left(\frac{\tau-N(P_3-P_2)}{\sqrt{N(P_3-P_2)(1-P_3+P_2)}}\right)$	$Q\left(\frac{N(P_3-P_2+P_1)-\tau}{\sqrt{N((P_3-P_2)(1-P_3+P_2)+P_1(1-P_1))}}\right)$
1	1	$Q\left(\frac{\tau-N(P_3-P_1)}{\sqrt{N(P_3-P_1-(P_2-P_1)^2-(P_3-P_2)^2)}}\right)$	$Q\left(\frac{NP_3-\tau}{\sqrt{N(P_3-P_1^2-(P_2-P_1)^2-(P_3-P_2)^2)}}\right)$

where $j = 1, 2, ..., 2^I$, is the error pattern index. $P(N_{c,j} > \tau)$ is the probability of $N_{c,j} > \tau$. Here the transmitted probabilities of '0' and '1' are assumed as 0.5 and 0.5 respectively.

Conversely, the error probability for the second case can be obtained by:

$$P_{10,j} = \frac{1}{2^I} P\left(N_{c,j} \leq \tau\right)$$
$$= \frac{1}{2^I} P\left(\sum_{i=0}^{I} a_{c-i,j} N_i \leq \tau\right). \tag{9}$$

Thus, the error probability for an un-coded system is given as:

$$P_{uc} = \frac{1}{2} \sum_{j=1}^{2^I} \left(P_{01,j} + P_{10,j}\right). \tag{10}$$

Table 1 give examples of different error patterns and error probabilities when $I = 2$, and $Q(\cdot)$ is the Q-function defined as:

$$Q(x) = \frac{1}{2}\text{erfc}\left(\frac{x}{\sqrt{2}}\right). \tag{11}$$

As can be seen in Figure 4, for a given distance $r = 15$ μm, the longer the ISI length I, the higher the BER. It can also be noted that as the ISI length increases, its effect on the BER becomes less prominent, i.e. the BER value begins to converge.

3. Energy Model

Introducing coding techniques can improve the performance of the communication system, however there will be an extra cost in energy due to the encoding and decoding processes at the T_X and R_X. This extra energy is proportional to the complexity of the encoder and decoder circuits. The energy required could be achieved through the use of smart nano-materials, such as piezoelectric nano-generators, based for example on arrays of nanowires (usually zinc-oxide) that could harvest sufficient mechanical energy to power the communications system (or the T_X) [30]. Additional possibilities could also be explored in the future for this purpose such as the use of a trioboelectric nano-generators, a pyroelectric nano-generators, or an optoelectronic nano-generators [31], [32], [33].
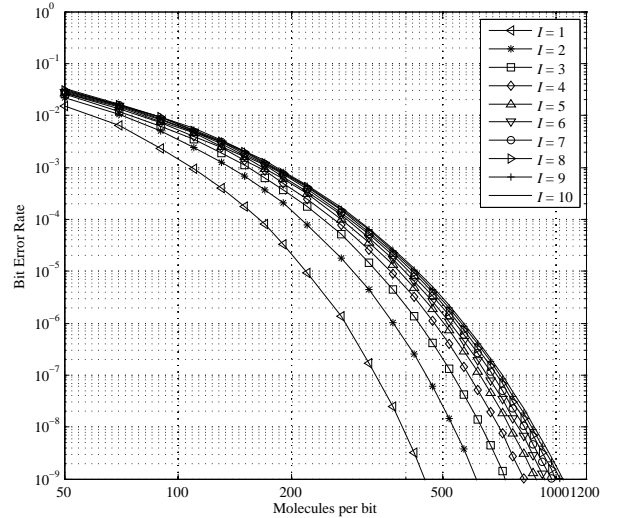

Figure 4: The BER with number of molecules per bit for un-coded system with different ISI length, $I = 1$ to 10, $r = 15$ μm
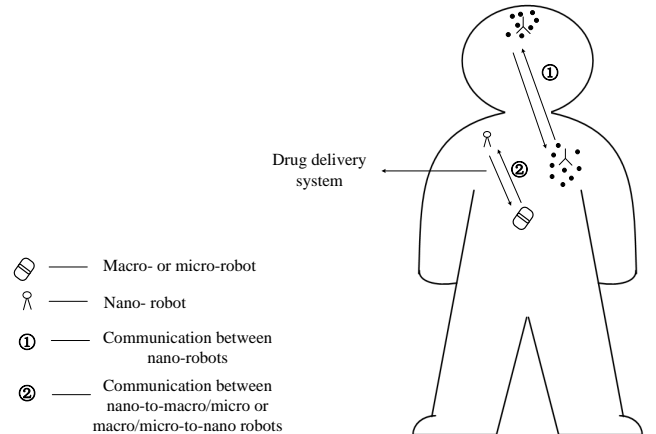

Figure 5: The communication schemes of intra-body nano-networks.

In Section 1, it was mentioned that the most pertinent application is as an intra-body network that collects and monitors vital biological activity [6]. In the healthcare domain, the quality of the data and the energy efficiency are two key metrics for the analysis process. Figure 5 illustrates some communication processes used in medical applications. For nano-to-nano robot communication, the extra energy requirements introduced by the encoder and decoder need to be taken into account. However, there may be other applications where the complexity of the two robots is not similar. For example, in drug delivery systems, a set of nano-robots as the beacons located around the body can transmit information to guide macro- or micro- scale drug delivery robots working around human blood vessels [34], [35]. In this case, the T_Xs are

considered much simpler than the R_Xs, so when calculating the energy, only the encoding processing needs to be taken into account. Conversely, there might be applications that need the R_X to be much simpler than the T_X so only the decoding process needs to be included in energy calculations.

Adenosine triphosphate (ATP) [36] is used to measure the energy transfer between cells in living organisms, and in this work, it is used to calculate the energy requirements of the proposed coding systems. The authors in [37] and [38] stated that one switch of a NAND gate will cost one ATP, where one ATP approximately equals $20K_BT$, where K_B is the Boltzmann constant, and the system is assumed to operate at an absolute temperature of $T = 300K$. Considering that NAND gates are well known as a universal gates, all further logic circuits can be constructed through their use. In this work, NOT gates, AND gates and XOR gates can be formed by using one, two and four NAND gates respectively. Each shift register unit used here is a SR (set-reset) flip-flop, and each can be constructed using four NAND gates. In this model, the code generation molecules are also required to encode and decode the data [39], and these molecules assumed to be distinct from the information molecules, as they are only used as internal molecules within the T_X and R_X and are not be affected by diffusion. The energy consumed by a T_X synthesizing a code generation molecule is approximately $2450K_BT$ [29], so for a given number of such molecules, the energy used for their synthesis can be computed. Thus, for a given encoder or decoder circuit, the total energy consumption can be separated into two parts, the energy consumption for synthesizing the code generation molecules and the energy consumption for the operation of logic gates. The detailed calculations for the selected ECCs will be given in Section 4. Furthermore, in this work, the energy measurements are scaled by K_BT.

4. Error Correction Coding Techniques

Two classes of codes in common use today are presented in this paper, which are block codes such as Hamming codes, and convolutional codes such as SOCCs. Each will be discussed in turn.

4.1. Hamming Codes

A Hamming code is one of the simple linear block codes used in many applications, denoted as (n_H, k_H) where $n_H = 2^m - 1$ is the block length ($m \geq 2$), and $k_H = n_H - m$, is the information length. Block codes can correct t errors in each block:

$$t = \lfloor (d_{min} - 1) \rfloor / 2, \qquad (12)$$

where $\lfloor x \rfloor$ returns to the largest integer not greater than x, and $d_{min} = 3$ is the minimum distance of Hamming codes. Therefore, Hamming codes can correct one error in each block.

(a) Non-systematic encoder
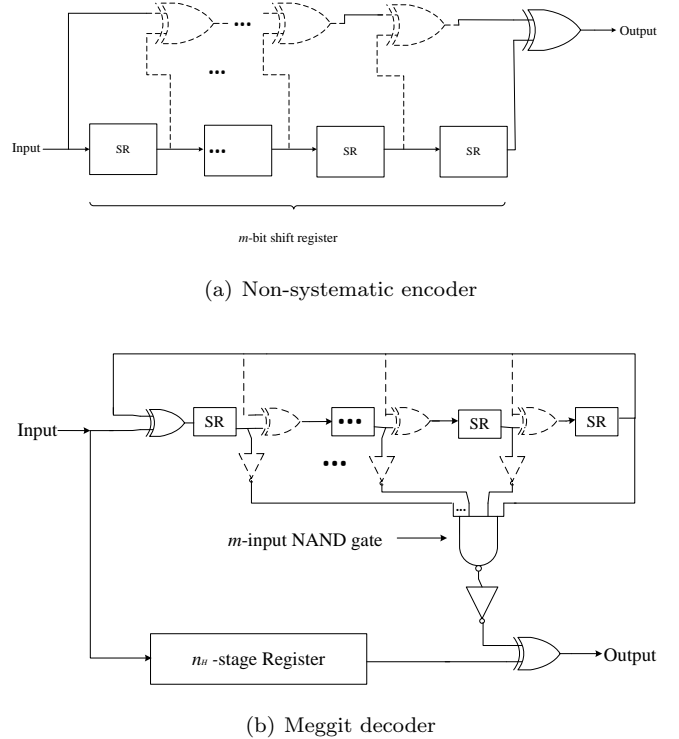

(b) Meggit decoder

Figure 6: General non-systematic encoder and Meggit decoder design for a Hamming code [40, Figure 8.13, Figure 8.19].

In this work, the Hamming codes considered are cyclic Hamming codes [40] which can be easily encoded by multiplying the information polynomial with the generator polynomials. This encoding process can be realized using a non-systematic encoder whilst the encoded message can be decoded using a Meggit decoder [40].

Here Hamming codes with $m \in \{3, 4, 5\}$ are considered for this proposed system. Figure 6 shows the general encoder and decoder designs for a Hamming code.

In order to compare the coded and un-coded system performance, the BER for the coded case needs to be determined. When considering a block code with t error correcting capability employed in the system, if the decoder can correct all combinations of errors less than or equal to t, but no combinations of errors greater than t, the BER of the coded system is illustrated in [41, Equation 6.46]. Here, the BER, P_{c-H}, can be approximated as:

$$P_{c-H} \approx \frac{1}{n_H} \sum_{j=t+1}^{n_H} j \binom{n_H}{j} {P'_{uc}}^{j} (1 - P'_{uc})^{n_H - j}, \qquad (13)$$

where P'_{uc} is the corresponding one-bit error probability. In order to use the same number of molecules as an un-coded system, P'_{uc} should be evaluated with a reduction in the number of molecules used for an un-coded system, (10), by multiplying with the code rate of the corresponding ECC.

Combining the ATP energy model introduced in Section 3, a NOT, XOR gate, and shift register unit will cost

5

one, four, and four ATPs respectively. It will also be assumed that a multi-input NAND gate will require only one ATP [13]. Therefore, with reference to Figure 6, for $m \in \{3, 4, 5\}$ Hamming codes, two XOR gates and m shift registers are needed for each circuit of the encoder which implies the energy cost of encoding is:

$$E_{encode-H} = 20N_{\text{tx}}(4m + 8) + 2450N_{\text{tx}}, \qquad (14)$$

where N_{tx} are the number of code generation molecules need for the coding process in the transmitter. Three XOR gates, $(m + n_H)$ shift registers, $(m - 1)$ NOT gates and one multi-input NAND gate are needed for each decoder circuit which implies the energy cost of the Meggit decoder is:

$$E_{decode-H} = 20N_{\text{rx}}(5m + 4n_H + 12) + 2450N_{\text{rx}}, \quad (15)$$

where N_{rx} are the number of code generation molecules for the decoding process in the receiver. In order to reduce the effects that come from the biochemical intrinsic distortion, it is assumed that $N_{\text{tx}} = N_{\text{rx}} = 300$ [13].

4.2. SOCCs

The convolutional code considered here is the SOCC which can be easily decoded using a majority-logic decoding scheme. For an (n_s, k_s, b) SOCC, n_s is the code length, k_s is the information length and b is the number of input memory blocks. $R_s = k_s/n_s$ is the code rate [22]. In this work, only SOCCs with an information length $k_s = n_s - 1$ are considered.

This paper represents four SOCCs: they are $(2, 1, 6)$ and $(2, 1, 17)$ SOCCs, both with $R_s = 1/2$, and $(3, 2, 2)$ and $(3, 2, 13)$SOCCs, both with $R_s = 2/3$. The generator polynomials of $(2, 1, 6)$SOCC and $(2, 1, 17)$SOCC are:

$$g_1^{(2)}(D) = 1 + D^2 + D^5 + D^6, \qquad (16)$$

$$g_1^{(2)}(D) = 1 + D^2 + D^7 + D^{13} + D^{16} + D^{17}. \qquad (17)$$

where $g_i^{(n_s)}$ is the generator polynomial with $i = 1, 2, ..., k_s$.

For $(3, 2, 2)$SOCC, a pair of generator polynomials are:

$$g_1^{(3)}(D) = 1 + D, \qquad (18)$$
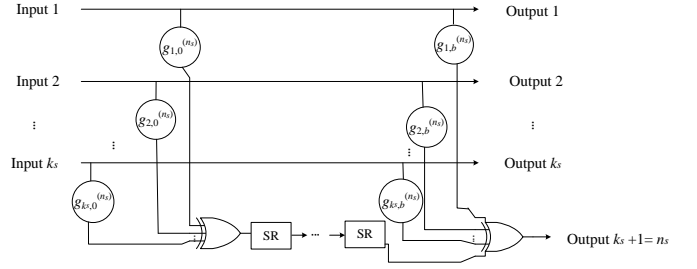
$$g_2^{(3)}(D) = 1 + D^2. \qquad (19)$$

For $(3, 2, 13)$SOCC, a pair of generator polynomials are:

$$g_1^{(3)}(D) = 1 + D^8 + D^9 + D^{12}, \qquad (20)$$

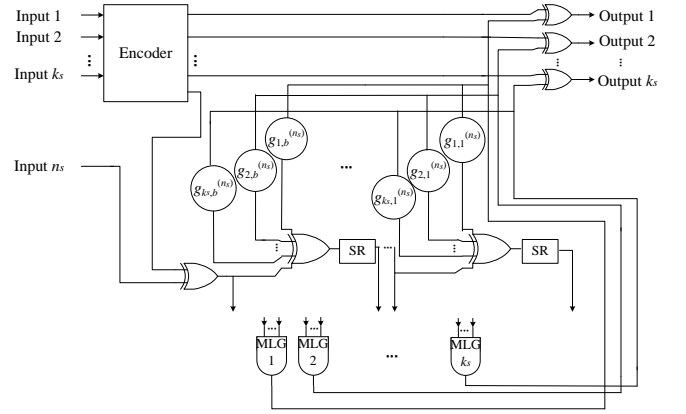$$g_2^{(3)}(D) = 1 + D^6 + D^{11} + D^{13}. \qquad (21)$$

The maximum BER (which is the worst performance case) of SOCCs with a feedback majority-logic decoder can be upper bounded by [22, Equation 13.42]:

$$P_{cmax-S} = \frac{1}{k_s} \sum_{i=t_{ML}+1}^{n_E} \binom{n_E}{i} P_{uc}'^i (1 - P_{uc}')^{n_E-i}, \qquad (22)$$

$g_{i,j}^{(n_s)}$: The coefficient of each term in the polynomial $g_i^{(n_s)}$
$\quad i = 1, 2, ..., k_s, \ j = 0, 1, ..., b.$

(a) Encoder

(b) Decoder

Figure 7: General encoder and decoder design for a (n_S, k_S, b) SOCC [22, Figure 13.5].

where $n_E = 1/2(J^2 + J)k_s + 1$ is the effective constraint length [21], $t_{ML} = \lfloor J/2 \rfloor$ is the majority-logic error-correcting capability, and J is the number of checksums orthogonal on one error.

Figure 7(a) gives a general encoder circuit for SOCC. The number of shift register units for the encoder is b, and number of XOR gates is dependent upon on the generator polynomials. The energy cost of the encoding is thus:

$$E_{encode-S(2,1,6)} = 20N_{\text{tx}}(4b + 12) + 2450N_{\text{tx}}, \qquad (23)$$

$$E_{encode-S(2,1,17)} = 20N_{\text{tx}}(4b + 20) + 2450N_{\text{tx}}, \qquad (24)$$

$$E_{encode-S(3,2,2)} = 20N_{\text{tx}}(4b + 12) + 2450N_{\text{tx}}, \qquad (25)$$

$$E_{encode-S(3,2,13)} = 20N_{\text{tx}}(4b + 28) + 2450N_{\text{tx}}. \qquad (26)$$

A general feedback majority-logic decoder for the SOCC is shown in Figure 7(b), which can be separated into two parts. One is the same as the encoder, and the other part contains b register units and k_s majority-logic gates (MLGs). The MLGs used here are two-input MLGs, where each one can be considered as an AND gate. The number of XOR gates is dependent on the polynomial generator and the information length. So the energy cost of the
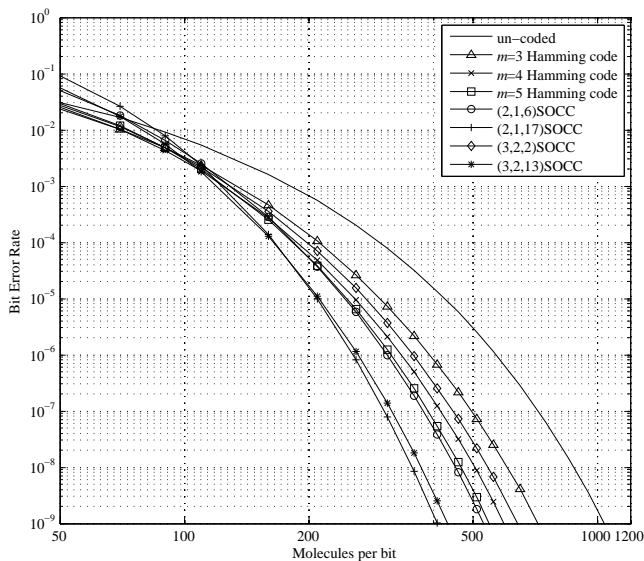
Figure 8: The BER performance for different coding techniques with molecules per bit at $r = 15$ μm with $I = 10$.

Table 2: The comparison of values of coding gain for Hamming codes and SOCCs. 'H' represents Hamming code, 'S' represents SOCC.

BER level	$m = 3$ H	$m = 4$ H	$m = 5$ H	(2,1,6) S	(2,1,17) S	(3,2,2) S	(3,2,13) S
10^{-9}	1.58dB	2.41dB	2.77dB	2.92dB	4.03dB	2.08dB	3.78dB
10^{-3}	1.30dB	1.64dB	1.60dB	1.47dB	1.68dB	1.44dB	1.82dB

decoding is:

$$E_{decode-S(2,1,6)} = 20N_{\mathrm{rx}}(8b + 37) + 2450N_{\mathrm{rx}}, \quad (27)$$

$$E_{decode-S(2,1,17)} = 20N_{\mathrm{rx}}(8b + 70) + 2450N_{\mathrm{rx}}, \quad (28)$$

$$E_{decode-S(3,2,2)} = 20N_{\mathrm{rx}}(8b + 36) + 2450N_{\mathrm{rx}}, \quad (29)$$

$$E_{decode-S(3,2,13)} = 20N_{\mathrm{rx}}(8b + 74) + 2450N_{\mathrm{rx}}. \quad (30)$$

5. Numerical Results

The performance of coding techniques in molecular communication systems is evaluated via two aspects: one is the BER, and the other is the energy consumption. In this work, $R = 5$ μm, $D = 79.4$ μm^{2}s^{-1} and $I = 10$.

Figure 8 provides the BER compared with an un-coded system and a coded system that employs Hamming codes and SOCCs at a distance of $r = 15$ μm, and $t_s = 2.2899$ s. The BERs for the un-coded and coded systems can be obtained through the evaluation of equations (10), (13), and (22).

Here the coding gain is introduced as an easy way to measure the BER performance. It can be directly obtained as:

$$G_{coding} = 10 \times \log\left(\frac{N_{uncoded}}{N_{coded}}\right), \quad (31)$$

where $N_{uncoded}$ and N_{coded} are the number of molecules for an un-coded and coded system at a chosen BER level.

From the BER performance results shown in Figure 8, increasing the number of molecules per bit leads to a smaller BER for un-coded and coded system. Values of the coding gain of Hamming codes and SOCCs are shown in Table 2. It indicates that for the system that requires a lower BER, the (2,1,17)SOCC provides the highest system performance. This is because the (2,1,17)SOCC has the highest correcting capability among these coding schemes.

As discussed in Section 3, this increase in performance will cost energy. The energy saving (or loss) ΔE for a coded molecular communication system is defined as [13, Equation 7]:

$$\Delta E = E_{uncoded} - E_{coded}, \quad (32)$$

where $E_{uncoded}$ and E_{coded} are the energy requirements for un-coded and coded systems, and can be constructed as:

$$E_{uncoded} = 2450N_{uncoded}, \quad (33)$$

$$E_{coded} = 2450N_{coded} + E_{encode} + E_{decode}. \quad (34)$$

Therefore, ΔE can be written as:

$$\Delta E = 2450\left(N_{uncoded} - N_{coded}\right) - E_{encode} - E_{decode}, \quad (35)$$

where E_{encode} and E_{decode} are the energy requirements for the encoding and decoding processes.

It is therefore easy to see that when $\Delta E \geq 0$, the use of ECC is beneficial to the molecular communication system. Thus, the critical case, $\Delta E = 0$ is thus important for determining whether the ECC is suitable for molecular communication system. In this case, (35) can be reduced to:

$$N_{uncoded} - N_{coded} = \left(E_{encode} + E_{decode}\right)/2450. \quad (36)$$

Here, the critical distance r_0 [14] is introduced as a metric to determine when the use ECCs becomes beneficial. It is defined as the distance (between the centre of the T$_X$ and the centre of the R$_X$) at which the coding gain matches the extra energy requirements introduced by the ECCs. It can also be considered as the distance to satisfy the critical case (36). The relationship between $N_{uncoded}$ and N_{coded} can be easily obtained by substituting the energy consumption values for different coding schemes in (14), (15), in (23) through (30). In this work, the critical distance r_0 has been proposed for choosing the best-fit ECC for the molecular communication system. As is shown in (36), the r_0 can be affected by BER performance and the complexity.

Figures 9,10,11 show the critical distance r_0 for different coding techniques. Based on the scenarios introduced in Section 3, the results will be discussed over a BER range of 10^{-9} to 10^{-3}. These figures clearly show which code is better for the given parameters. For a specific operating BER, when the transmission distance is longer than r_0, this code is suitable for this system. The results also indicate that the coding techniques are beneficial for longer range transmission systems. In addition, for all kinds of scenarios, the critical distance increases with increasing BER for all codes.

7
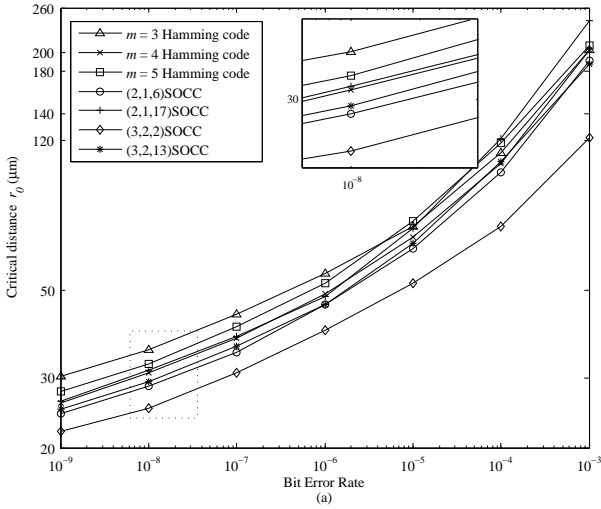
0.95

Figure 9: Critical distance r_0 for coded system with BER for $m = \{3, 4, 5\}$ Hamming codes, and $(2, 1, 6), (2, 1, 17), (3, 2, 2)$ and $(3, 2, 13)$SOCCs.
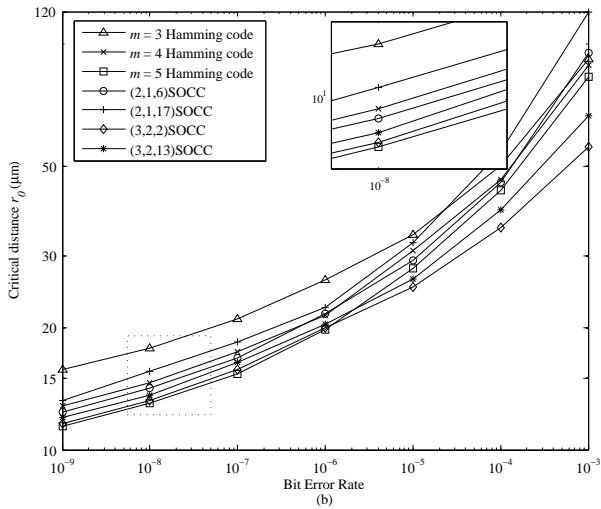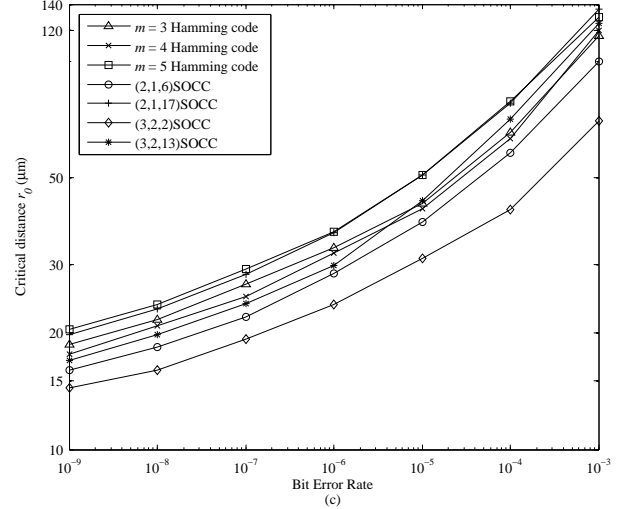

0.95

Figure 10: Critical distance r_0 for coded system with BER for $m = \{3, 4, 5\}$ Hamming codes, and $(2, 1, 6), (2, 1, 17), (3, 2, 2)$ and $(3, 2, 13)$SOCCs when only the transmission process energy is considered.

Figure 9 considers the r_0 for nano-to-nano device communication. In this case, both the encoding and decoding processes at the T_X and R_X need to be considered. The lowest distance is given by the use of the $(3, 2, 2)$SOCC, which means that $(3, 2, 2)$SOCC has a wider application range.

Figure 10 and Figure 11 show other scenarios which are the nano-to-macro device communication and macro-to-nano device communication. When considering nano-to-macro device communication, the energy cost only in-

0.95

Figure 11: Critical distance r_0 for coded system with BER for $m = \{3, 4, 5\}$ Hamming codes, and $(2, 1, 6), (2, 1, 17), (3, 2, 2)$ and $(3, 2, 13)$SOCCs when only the receiving process energy is considered.

cludes the encoding process at the T_X by setting $E_{decode} = 0$ in (36). For macro-to-nano device communication, the E_{encode} set to zero in (36). Under these conditions, the level of critical distance decreases compared with the nano-to-nano device communication. The lowest critical distance belongs to the $m = 5$ Hamming code and $(3, 2, 2)$SOCC.

6. Conclusions

In this paper, Hamming codes and SOCCs have been introduced into the molecular communication system, and the performance enhancements of SOCCs have been compared against Hamming codes with regards to both the coding gain and energy requirements. The results show that the coding techniques do enhance the performance of the molecular communication system. In addition, the $(2, 1, 17)$SOCC is more energy efficient when low BERs are required.

To choose the coding techniques for different communication scenarios, the critical distance as a performance metric is also evaluated. The critical distance is measured by defining the distance at which the use of coding becomes beneficial. It has been indicated that an increase of the operating BER results in a longer critical distance. For nano-to-macro and macro-to-nano device communications, the critical distance decreases in comparison with nano-to-nano device communication. Moreover, for a system with a specific operating BER and transmission distance, the most suitable code can be selected by analysing these performance metrics.

8

References

[1] Akyildiz IF, Jornet JM. The Internet of nano-things. IEEE Wireless Communications 2010; 17(6):58–63. doi: 10.1109/MWC.2010.5675779.

[2] LaVan DA, McGuire T, Langer R. Small-scale systems for in vivo drug delivery. Nature Biotechnology 2003; 21(10):1184–1191. doi:10.1038/nbt876.

[3] Leary SP, Liu CY, Apuzzo ML. Toward the emergence of nanoneurosurgery: part III–nanomedicine: targeted nanotherapy, nanosurgery, and progress toward the realization of nanoneurosurgery. Neurosurgery 2006; 58(6):1009–1026. doi: 10.1227/01.neu.0000217016.79256.16.

[4] Akyildiz IF, Biunetti F, Blázquez C. Nanonetworks: A new communication paradigm. Computer Networks 2008; 52(12):2260–2279. doi:10.1016/j.comnet.2008.04.001.

[5] Bush SF, Paluh JL, Piro G,Rao V,Prasad RV,Eckford A. Defining Communication at the Bottom. IEEE Transactions on Molecular, Biological and Multi-Scale Communications 2015; 1(1):90–96. doi:10.1109/TMBMC.2015.2465513.

[6] Balasubramaniam S, Kangasharju J. Realizing the Internet of Nano Things: Challenges, Solutions, and Applications. Computer 2013; 46(2):62–68. doi:10.1109/MC.2012.389.

[7] Miorandi D, Sicari S, De Pellegrini F, Chlamtac I. Internet of things: Vision, applications and research challenges. Ad Hoc Networks 2012; 10(7):1497–1516. doi: 10.1016/j.adhoc.2012.02.016.

[8] Zorzi M, Gluhak A, Lange S, Bassi A. From today's INTRAnet of things to a future INTERnet of things: a wireless- and mobility-related view. IEEE Wireless Communications 2010; 17(6):44–51. doi:10.1109/MWC.2010.5675777.

[9] Iera A, Floerkemeier C, Mitsugi J, Morabito G. The Internet of things [Guest Editorial]. IEEE Wireless Communications 2010; 17(6):8–9. doi: 10.1109/MWC.2010.5675772.

[10] Jornet JM, Akyildiz IF. Joint Energy Harvesting and Communication Analysis for Perpetual Wireless Nanosensor Networks in the Terahertz Band. IEEE Transactions on Nanotechnology 2012; 11(3):570–580. doi:10.1109/TNANO.2012.2186313.

[11] Dressler F, Kargl F. Towards security in nano-communication: Challenges and opportunities. Nano Communication Networks 2012; 3(3):151–160. doi:10.1016/j.nancom.2012.08.001.

[12] Leeson MS, Higgins MD. Error correction coding for molecular communications. In: IEEE International Conference on Communications (ICC). IEEE; 2012, 6172–6176. doi: 10.1109/ICC.2012.6364980.

[13] Leeson MS, Higgins MD. Forward error correction for molecular communications. Nano Communication Networks 2012; 3(3):161–167. doi:10.1016/j.nancom.2012.09.001.

[14] Howard SL, Schlegel C, Iniewski K. Error control coding in low-power wireless sensor networks: When is ECC energy-efficient?. EURASIP Journal on Wireless Communications and Networking 2006; 2:1–14. doi:10.1155/WCN/2006/74812.

[15] Shih PJ, Lee CH, Yeh PC, Chen KC. Channel Codes for Reliability Enhancement in Molecular Communication. IEEE Journal on Selected Areas in Communications 2013; 31(12):857–867.

[16] Lu Y, Higgins MD, Leeson MS. Diffusion based molecular communications system enhancement using high order hamming codes. In: 9th International Symposium on Communication Systems, Networks Digital Signal Processing (CSNDSP). IEEE; 2014, 438–442. doi:10.1109/CSNDSP.2014.6923869.

[17] Bai CY, Leeson MS, Higgins MD. Minimum energy channel codes for molecular communications. Electronics Letters 2014; 50(23):1669–1671. doi:10.1049/el.2014.3345.

[18] Lu Y, Higgins MD,Leeson MS. Comparison of Channel Coding Schemes for Molecular Communications Systems. IEEE Transactions on Communications 2015; 63(11):3991–4001. doi: 10.1109/TCOMM.2015.2480752.

[19] Ganesan K, Grover P, Rabaey J. The power cost of over-designing codes. In: IEEE Workshop on Signal Processing Systems (SiPS). IEEE; 2011, 128–133. doi: 10.1109/SiPS.2011.6088962.

[20] Grover P, Sahai A. Green codes: Energy-efficient short-range communication. In: IEEE International Symposium on Information Theory(ISIT). IEEE; 2008, 1178–1182. doi: 10.1109/ISIT.2008.4595173.

[21] Bougeard S, Helard JF, Citerne J. A new algorithm for decoding concatenated CSOCs: application to very high bit rate transmissions. In: IEEE International Conference on Personal Wireless Communication. IEEE; 1999, 399–403. doi: 10.1109/ICPWC.1999.759657.

[22] Lin S, Costello DJ. Error control coding: fundamentals and applications. Prentice-Hall; 1983.

[23] Kavehrad M. Implementation of a self-orthogonal convolutional code used in satellite communications. IEE Journal on Electronic Circuits and Systems 1979; 3(3):134–138. doi:10.1049/ij-ecs.1979.0024.

[24] Townsend R, Weldon E. Self-orthogonal quasi-cyclic codes. IEEE Transactions on Information Theory 1967; 13(2):183–195. doi:10.1109/TIT.1967.1053974.

[25] Lu Y, Higgins MD, Leeson MS. Self-orthogonal convolutional codes (SOCCs) for diffusion-based molecular communication systems. In: IEEE International Conference on Communications(ICC). IEEE; 2015, 1049–1053. doi: 10.1109/ICC.2015.7248461.

[26] Yilmaz HB, Chae CB. Arrival modelling for molecular communication via diffusion. Electronics Letters 2014; 50(23):1667–1669. doi:10.1049/el.2014.2943.

[27] Ziff RM, Majumdar SN, Comtet A. Capture of particles undergoing discrete random walks. The Journal of Chemical Physics 2009; 130(20):204104. doi: http://dx.doi.org/10.1063/1.3137062.

[28] Kuran MŞ, Yilmaz HB, Tugcu T, Akyildiz IF. Modulation Techniques for Communication via Diffusion in Nanonetworks. In: IEEE International Conference on Communications(ICC). IEEE; 2011, 1–5. doi:10.1109/icc.2011.5962989.

[29] Kuran MŞ, Yilmaz HB, Tugcu T, Özerman B. Energy model for communication via diffusion in nanonetworks. Nano Communication Networks 2010; 1(2):86–95. doi: 10.1016/j.nancom.2010.07.002.

[30] Wang XD. Piezoelectric nanogeneratorsHarvesting ambient mechanical energy at the nanometer scale. Nano Energy 2012; 1(1):13–24. doi: http://dx.doi.org/10.1016/j.nanoen.2011.09.001.

[31] Wang ZL. Triboelectric nanogenerators as new energy technology and self-powered sensors - Principles, problems and perspectives. Faraday Discussions 2014; 176:13–24. doi: 10.1039/C4FD00159A.

[32] Lingam D, Parikh AR, Huang JC,Jain A,Minary-Jolandan M. Nano/microscale pyroelectric energy harvesting: challenges and opportunities. International Journal of Smart and Nano Materials 2013; 4(4):229–245. doi:10.1080/19475411.2013.872207.

[33] Lin YF, Song JH, Ding Y,Lu SY,Wang ZL. Alternating the Output of a CdS Nanowire Nanogenerator by a White-Light-Stimulated Optoelectronic Effect. Advanced Materials 2008; 20(16):3127–3130. doi:10.1002/adma.200703236.

[34] Thombre AG, Cardinal JR, DeNoto AR, Herbig SM, Smith KL. Asymmetric membrane capsules for osmotic drug delivery: I. Development of a manufacturing process. Journal of Controlled Release 1999; 57(1):55–64. doi: http://dx.doi.org/10.1016/S0168-3659(98)00100-X.

[35] Nain S, Sharma NN. Propulsion of an artificial nanoswimmer: a comprehensive review. Frontiers in Life Science 2014; 8(1):2–17. doi:10.1080/21553769.2014.962103.

[36] Nelson DL, Lehninger A, Cox MM, Osgood M, Ocorr K. Lehninger Principles of Biochemistry / The Absolute, Ultimate Guide to Lehninger Principles of Biochemistry. Macmillan Higher Education; 2008.

[37] Sauro HM, Kholodenko BN. Quantitative analysis of signaling networks. Progress in biophysics and molecular biology 2004; 86(1):5–43. doi:10.1016/j.pbiomolbio.2004.03.002.

[38] Shacter E, Chock PB, Stadtman ER. Energy consumption in a cyclic phosphorylation/dephosphorylation cascade. Journal of

Biological Chemistry 1984; 259(19):12260–12264.

[39] Levine J, Kueh HY, Mirny L. Intrinsic fluctuations, robustness, and tunability in signaling cycles. Biophysical Journal 2007; 92(12):4473–4481. doi:10.1529/biophysj.106.088856.

[40] Blahut RE. Algebraic Codes for Data Transmission. Cambridge University Press; 2003.

[41] Sklar B. Digital communications: fundamentals and applications. Prentice-Hall PTR; 2001.

Yi Lu received the degree of Bachelor of Engineering with First Class Honors in Electronic Engineering from University of Central Lancashire, UK, in 2011. And then she obtained a Master degree of Engineering with Distinction in Electronic Engineering from University of Sheffield, UK, in 2012. She is currently a scholarship student pursuing a PhD study in Nano-communications at University of Warwick.

Xiayang Wang received the degree of Bachelor of Science majoring in Opto-information Science and Technology from the Department of Optoelectronics Science and Technology in Huazhong University of Science and Technology, China, in 2011. In 2013, he graduated from the Department of Electronics at the University of York, receiving a First Class Honors MSc degree in Communications Engineering. Xiayang then moved to the University of Warwick where he obtained his PhD in Nano-communications in 2016.

Matthew D. Higgins received his MEng in Electronic and Communications Engineering and his PhD in Engineering from the School of Engineering at the University of Warwick in 2005 and 2009 respectively. Remaining at the University of Warwick, he then progressed through several Research Fellow positions, in association with some of the UKs leading defence and telecommunications companies. In July 2012, Dr Higgins was promoted to the position of Assistant Professor where his research focused on Optical, Nano, and Molecular Communications. Whilst is this position, Dr Higgins set up the Vehicular Communications Research Laboratory. As of March 2016, Dr Higgins was appointed as an Associate Professor at WMG working in the area of Connected and Autonomous Vehicles. Dr Higgins is a Senior Member of the IEEE, *SMIEE*.

Adam Noel received the B.Eng. degree in Electrical Engineering in 2009 from Memorial University in St. John's, Canada, the M.A.Sc. degree in Electrical Engineering in 2011 from the University of British Columbia (UBC) in Vancouver, Canada, and the Ph.D. degree in Electrical and Computer Engineering in 2015 from UBC. In 2013 he was a Visiting Scientist at the Institute for Digital Communication at Friedrich-Alexander-University in Erlangen, Germany. He is currently a Postdoctoral Fellow at the University of Ottawa in Ottawa, Canada. Dr. Noel's current research interests include channel modelling, system design, and simulation methods for molecular communication networks. He is a Member of the IEEE.
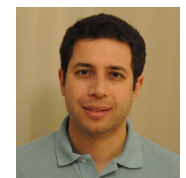
Neophytos Neophytou received his PhD in Electrical and Computer Engineering from Purdue University, West Lafayette, IN, USA in 2008. He worked as a Post-Doctoral Researcher at the Institute of Microelectronics at the Technical University of Vienna in Austria until 2013. He is currently an Associate Professor at the University of Warwick in the UK. His area of specialisation is theory, computational modeling and simulation of transport in nanoelectronic materials and devices including nanowires, ultra thin-body devices, carbon nanotubes, and graphene nanoribbons. His current research interests include thermoelectric transport in nanostructured devices for energy conversion and generation applications.

Mark S. Leeson received the degrees of BSc and BEng with First Class Honors in Electrical and Electronic Engineering from the University of Nottingham, UK, in 1986. He then obtained a PhD in Engineering from the University of Cambridge, UK, in 1990. From 1990 to 1992 he worked as a Network Analyst for National Westminster Bank in London. After holding academic posts in London and Manchester, in 2000 he joined the School of Engineering at Warwick, where he is now a Reader in Communications Systems. His major research interests are coding and modulation, molecular communications and evolutionary optimisation. To date, Dr. Leeson has over 250 publications and has supervised 16 successful research students. He is a Senior Member of the IEEE, and a Fellow of both the UK Institute of Physics and the UK Higher Education Academy.